Liquid Metal Mass Flow Measurement by an Inductive Proximity Detector for Use in Conjunction with a J × B Pump

Michael A. Hepler,* William J. Coogan,* Brittany L. Ilardi†
and Edgar Y. Choueiri‡
Princeton University, Princeton, NJ, 08544, USA

A J × B feed system incorporating a variable magnetic field strength and translating inductive proximity detector has been designed to deliver and measure liquid metal mass flow rates in the range of 0 - 100 mg/s. Electric thruster research using metallic propellants under laboratory conditions requires sensitive control of low propellant mass flow rates. Previous mechanical and J × B systems have struggled to control and accurately measure flow rates less than 100 mg/s. Existing theory describing the behavior of J × B feed systems was applied to optimize the physical dimensions and magnetic field strength of a prototype J × B pump for low mass flow rate operation with liquid lithium. To meet the challenge of measuring the mass flow rate, an inductive proximity detector was incorporated to track the change in the propellant column height in the feed system reservoir to calculate the mass flow rate. Successful operation using liquid lithium was demonstrated for mass flow rates of 0.21-0.46 mg/s with a maximum error of ± 0.13 mg/s.

Nomenclature

B	Magnetic field strength
D	Tubing diameter between **J** × **B** pump and feed system output
f	Laminar friction coefficient
g	Gravitational acceleration
h	Column lift height to feed system output
j	Current density
J	Total current delivered to pump
k	Geometric loss coefficient
l	Tubing length between pump and feed system output
$\dot{m}$	Mass flow rate
P	Pressure
R_{res}	Reservoir radius
s	**J** × **B** pump channel height between magnets
v	Fluid velocity
μ	Coefficient of friction
ρ	Mass density
σ	Standard deviation

*Graduate Student, MAE Dept., Princeton University, AIAA Student Member.
†Undergraduate Student, MAE Dept., Princeton University.
‡Chief Scientist, EPPDyL, Professor, Applied Physics Group, MAE Dept., Princeton University, AIAA Fellow.

I. Introduction

The use of metallic propellants can be found in almost every category of electric thruster including magnetoplasmadynamic, electrostatic and hall thrusters, showing promise as a path toward long-lived, high-power electric propulsion.[1] To investigate these thrusters under laboratory settings, it is necessary to both control and measure mass flow rates under 100 mg/s.[2] A number of feed systems have been developed to deliver liquid metals in this low mass flow rate regime, yet each has faced considerable difficulties in implementation.

Mechanical feed systems have an advantage in that the piston motion shares a linear relationship with the mass flow rate. However, a number of failure modes make for unreliable performance during thruster firing. In the case of liquid lithium propellant delivery to MPD thrusters, the current state-of-the-art system lacks O-ring materials which can be used to prevent lithium from leaking from the top of the piston. The top of the piston is therefore actively cooled, freezing the lithium and forming a seal.[3] This frozen lithium must be sheared as the piston moves, and any freezing of lithium downstream results in large forces generated by the piston motor, producing pressures capable of bending the piston arm, creating leaks at the pipe joints, and damaging other feed system components.

Electromagnetic $\mathbf{J} \times \mathbf{B}$ pumps have also been designed as an option for delivering liquid metals at low mass flow rates. By passing a current through a conductive fluid in the presence of a magnetic field, a Lorentz force is generated and can be used to control the mass flow rate without moving components. Polzin and Markusic developed such a pump at NASA's Marshall Space Flight Center, successfully operating with gallium and bismuth in a closed loop configuration in the flow rate regime of 1 g/s and producing pump pressures up to 10 kPa.[1] However, these pumps were not implemented due to a lack of means by which to measure mass flow rates under 100 mg/s.[2]

Building on the work of Polzin and Marcusik,[1,2] a novel feed system using a $\mathbf{J} \times \mathbf{B}$ pump has been designed and tested using an inductive proximity detector to measure mass flow rates from 0 - 100 mg/s. The $\mathbf{J} \times \mathbf{B}$ pump has the distinct advantage of delivering liquid lithium without moving components at a constant pressure as opposed to a constant volumetric displacement used by the mechanical system, while the inductive proximity detector addresses the issue of measuring small mass flow rates previously encountered with $\mathbf{J} \times \mathbf{B}$ pumps.[2] A discussion of the design process is presented in Section II and validation of the feed system using liquid lithium is found in Section III.

II. System Design

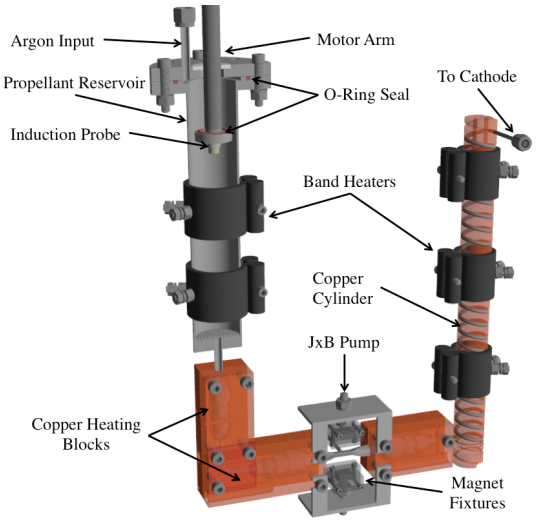

Figure 1. The feed system incorporates a $\mathbf{J} \times \mathbf{B}$ pump to deliver lithium to the thruster in conjunction with a high-temperature inductive proximity detector to track the mass flow rate. By attaching the inductive proximity detector to a linear piston motor, the changing propellant column height in the reservoir can be monitored, and the mass flow rate is obtained.

The feed system design took into account five main requirements: the ability to pump lithium, withstand and deliver lithium from the reservoir to the thruster, control and monitor the temperature, deliver mass flow rates of 0 - 100 mg/s, measure the mass flow rate, and isolate the reservoir from the environment during loading and priming the pump. In the following subsections we outline the design process and rationale for each requirement. A model of the final design is shown in Figure 1.

A. General Considerations

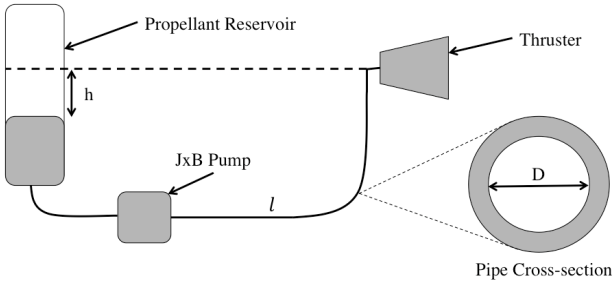

Figure 2. A diagram of the feed system is depicted. Here, h is the difference between the thruster and the lithium column height, and l refers to the length of tubing between the pump and the thruster.

To determine the necessary physical parameters for the feed system, a basic theoretical model of the pump was established. Following the analysis of Polzin and Markusic,[1] the force experienced by the conductive fluid due to the Lorentz interaction can be written as the volumetric integral

$$|\mathbf{F}| = \int \mathbf{j} \times \mathbf{B}\, d^3x, \tag{1}$$

where $\mathbf{j}$ is the current density, and $\mathbf{B}$ is the magnetic field strength. In the case of a rectangular pump channel and a constant magnetic field, the pressure can be written as

$$P = \frac{JB}{s}, \tag{2}$$

where J is the total applied current and s is the channel height between the magnets.[1] To understand the behavior of the $\mathbf{J} \times \mathbf{B}$ pump in the context of the entire feed system, this term can be included in Bernoulli's equation, giving

$$\rho g h + \frac{1}{2}\rho v^2 \left(1 + k + \frac{fl}{D}\right) - \frac{JB}{s} = 0, \tag{3}$$

which includes contributions from the column height, fluid flow, and Lorentz force. In the column height term, ρ is the fluid density, g is the gravitational acceleration and h is the difference between the thruster and column height. For the terms associated with the fluid flow, v is the fluid velocity, k is the friction coefficient due to geometric losses, f is the friction coefficient due to wall losses, l is the length of the tubing between the pump and thruster, and D is the tubing diameter. As we are looking at flow rates on the order of 10s to 100s of mg/s with a Reynolds number of ~ 100, we are well within the laminar flow regime and can write the friction coefficient due to wall interactions as[4]

$$f = \frac{64\mu}{\rho v D}, \tag{4}$$

where μ is the fluid viscosity. The value of μ was taken to be 6e-4 Pa·s for our investigations.[5] Additionally, as the feed system has no sharp turns, the geometric losses will have a negligible contribution, and the coefficient k can be neglected. By then substituting this expression into Eq. 3 and using mass continuity to obtain $\dot{m} = \rho v A$, where A is the pipe's cross-sectional area, the equation can be manipulated to arrive at an expression for the total applied current necessary to achieve a given mass flow rate:[6]

$$J = \frac{1}{B_s}\left[\frac{(\frac{4}{\pi}\dot{m} + 32\mu l)^2 - (32\mu l)^2}{2\rho D^4} + \rho g h\right], \tag{5}$$

where $B_s = B/s$. From Eq. 5 it was possible to investigate a range of system parameters in order to design a feed system which can operate in the chosen mass flow rate regime for a given propellant.

B. Application to Lithium

The feed system design for this paper was focused on the requirements of liquid lithium as our primary application is for a Lithium-fed Lorentz Force Accelerator (LiLFA). The primary issue involved with designing such a feed system is that the contribution due to the propellant column height easily dominates the current necessary to pump the fluid to the thruster at low mass flow rates of 0 - 100 mg/s. This means that a large current is necessary to lift the lithium to the thruster, but a fine current resolution is required to control the mass flow rate. The power supply for the $\mathbf{J} \times \mathbf{B}$ pump has a limited current output and resolution, and it was therefore necessary to match the desired range of mass flow rates with the range of output currents in order to maximize the mass flow rate resolution.

Several parameters of the system were constrained by available materials and equipment. For the pump, an Acopian model Y05LX7000 power supply was used with a current range of 0 - 70 A and a resolution of 100 mA. Additionally, the lift heights investigated were focused around the 150 mm range of the available piston motor used for moving the inductive proximity detector. Finally, based on available materials, stainless steel tubing was selected with an inner diameter of 2.06 mm. This tubing was selected as the first term in Eq. 5 has a strong inverse relationship to the piping diameter. By choosing smaller tubing, the required change in current to increase the mass flow rate rises.

With these constraints, the influence of the magnetic field strength, lift height, and tubing length on the pump mass flow rate resolution were investigated. By choosing these system parameters carefully, one can match the contributions of the J×B pump to that of the column height, thereby reducing the necessary current resolution to control the mass flow rate. To ensure that the pump can provide the maximum desired flow rate for any lithium column height in the feed system reservoir, it was necessary to find the minimum magnetic field strength required to achieve the maximum mass flow rate at the highest available current. For our experiments, this corresponds to a maximum mass flow rate of 100 mg/s and a maximum current of 58 A conducted through the lithium.

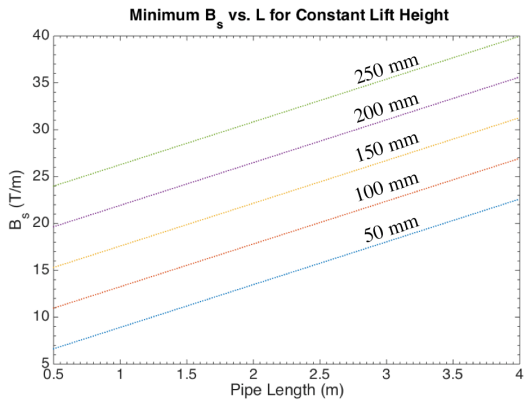

Figure 3. For a fixed tube diameter of 2.06 mm, the minimum value of B_s corresponding to a mass flow rate of 100 mg/s and a maximum current of 58 A conducted through the lithium is shown. This value was calculated over a range of maximum lift heights and pipe lengths.

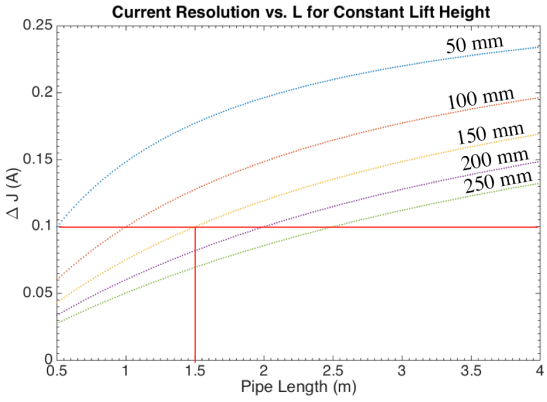

Figure 4. After calculating the minimum B_s value, the current resolution corresponding to a 0.5 mg/s change in the mass flow rate was calculated. This current resolution was determined for a number of maximum lift heights and pipe lengths. To meet the 100 mA current resolution of power supply, the piston which has a range of 150 mm required a minimum pipe length of 1.5 m.

By taking Eq. 5 and solving for B_s over a range of maximum lift heights and pipe lengths, the minimum B_s values were determined and is shown in Figure 3. Next, we needed to find the minimum current resolution required to meet the minimum mass flow rate resolution of $\Delta\dot{m} = 0.5$ mg/s for each of these lift heights and tubing lengths. To find this value, Eq. 5 was evaluated using the minimum change in mass flow rate and the minimum values of B_s giving the minimum current resolution of a given system configuration, found in Figure 4. From this figure, we find that, with a longer length of tubing and smaller lift heights, the $\Delta\dot{m}$ requirement can be fulfilled with the 100 mA resolution of the power supply. By reducing the lift height, less pressure is necessary to lift the propellant to the thruster. By lengthening the tubing, the frictional contribution to the total required current increases, and helps match the available current range to the

available current resolution. Using a reservoir height of 150 mm to fully utilize the range of the piston motor, a minimum tubing length of 1.5 m is required.

C. J × B Pump

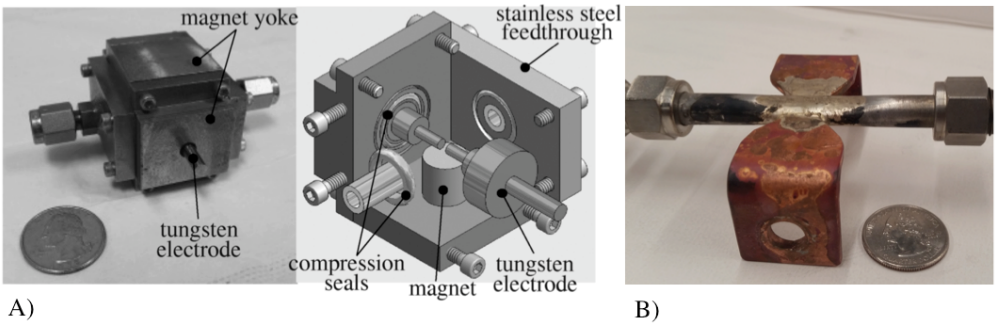

Figure 5. In photo A, the J × B pump developed by Polzin and Markusic is shown.[1] The pump volume is made of aluminum nitride and surrounded by a metal housing. While this system ensures that all current is directed through the liquid metal, the magnetic field strength is fixed and seals around the electrodes and stainless steel feedthroughs add complexity and possible leak points. The J × B pump developed for the new feed system is simplified, consisting of a flattened 3/4" stainless steel tube with electrodes braised directly to the body.

The feed system shown in Figure 1 employs an electromagnetic $\mathbf{J} \times \mathbf{B}$ pump, similar to the one designed by Polzin and Markusic. Their $\mathbf{J} \times \mathbf{B}$ pump design makes use of an aluminum nitride housing to insulate the electrodes and hold two permanent magnets at a fixed distance from one another.[1] Figure 5 shows Polzin and Markusic's design alongside the simplified pump we developed for the new feed system. The aluminum nitride housing ensures that all of the applied current passes directly through the liquid metal in the channel. Because tests using the previous $\mathbf{J} \times \mathbf{B}$ pump were carried out using gallium, which is about three times less conductive than lithium, it was necessary to direct all of the current directly through the liquid gallium to ensure efficient operation of the pump. However, we are primarily interested in lithium, and the increased conductivity allowed us to construct the pump body from stainless steel as more than 80% of the current will pass through the liquid metal. This design has a minimum number of potential propellant leak points, and allows for external magnets to be easily mounted in a configuration that can be manipulated. To prevent "vapor lock" from occurring during trials at vacuum, in which the pump volume was emptied and pumping ceased, the pump height between the magnets was made to be 9.5mm. This increased the pump volume allowing lithium to flow more readily into the pump, and decreased the force density within the pump.

D. System Heating

Due to the small diameter and increased length of the tubing, heating was a primary design consideration as any unheated sections of pipe could easily allow a freeze to take place, blocking the flow of lithium. As shown in Figure 1, the new feed system incorporates a number of copper heating blocks with redundant cartridge heaters to prevent freezing due to the failure of a single heating element. These copper blocks distribute heat uniformly over the length of the tubing making temperature monitoring possible with relatively few thermocouples. In order to accommodate the additional tubing length within a limited footprint, a heated copper cylinder was constructed. The tubing is wound into a recessed spiral groove and held in place by band heaters. Redundant heating of the reservoir and copper cylinder was achieved using multiple band heaters.

E. Mass Flow Rate Measurement

To measure mass flow rates in the desired range of 0 - 100 mg/s, a number of methods were considered. A similar $\mathbf{J} \times \mathbf{B}$ mass flow detector could be built to measure the mass flow rate of the propellant. By passing a conductive fluid through a magnetic field, a voltage is generated and could be measured and correlated to the mass flow rate. However, the desired range of mass flow rates would correspond to voltages too small to

be detected in the presence of the thruster arc.[2] Instead, a linear piston motor was fitted with a proximity detector to monitor the changing height of the lithium column surface.

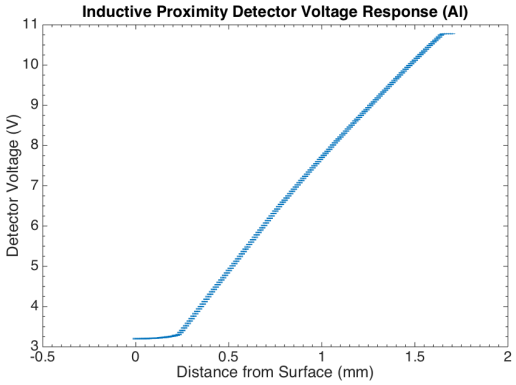

Figure 6. A high-temperature inductive proximity detector was selected for use in the lithium reservoir which regularly operates at 200°C. To calibrate the voltage response, the proximity detector was placed against the surface of the metal and a series of voltage measurements were taken as the detector was lifted from the surface. Here, a calibration of an aluminum surface is shown with an uncertainty $\sigma = \pm$ 0.016 V.

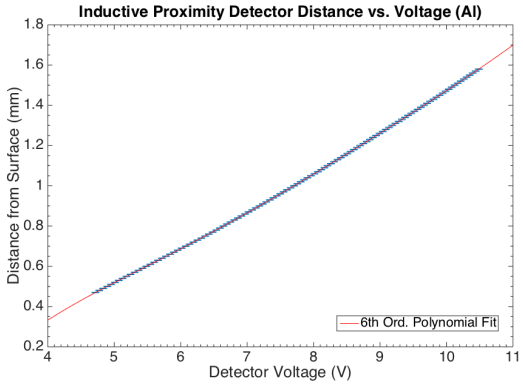

Figure 7. Once the voltage response of the proximity detector is found, a sixth-order polynomial fit relating the distance to the detector voltage is made to the near-linear region. In the case of aluminum, this fit was made from 4.7 V to 10.5 V with a uncertainty in distance of $\pm$ 0.003 mm.

For the final design, a General Electric model 3300 8MM inductive proximity detector was selected as it is capable of detecting the surface of the lithium without physical contact and is rated to 220°C, above the 180°C lithium melting temperature. The inductive proximity detector is attached to the linear piston motor which then moves the detector to track the reservoir column height using a control program. As the column height changes, the program moves the piston to a specified distance above the surface, and then holds the piston stationary. During this time, the distance to the surface is monitored until the proximity detector tip measures a threshold distance above the surface, and the piston is once again moved. The corresponding change in piston position and proximity detector voltage is used to calculate the mass of lithium in the reservoir and the propellant mass flow rate.

To validate the proximity detector's operation a series of calibrations were done using an aluminum surface at atmospheric pressure and room temperature. Using the piston arm, the proximity detector was placed against the surface of the metal, and a series of data points were taken as the detector height increased. A representative voltage curve for aluminum is shown in Figure 6. A near-linear region was chosen and a fit was then made relating the detector voltage to a distance above the metal surface. In the case of the aluminum plate, Figure 7 shows the result of a fit using data points between 4.7 - 10.5 V. The uncertainty of the height measurement was $\pm$ 0.003 mm.

F. Reservoir Seal

The final important design consideration for the feed system was to isolate the reservoir from the external environment during installation and allowing an inductive proximity detector to be raised and lowered by the piston arm during operation. To address these requirements, a stainless steel back plate with a silicone O-ring was attached to the threaded rod supporting the inductive proximity detector. A diagram of the detector seal is shown in Figure 8. The threaded rod is free to move vertically relative to the piston arm, and an O-ring seal is made by backing the piston arm against a spring, providing an upward force which seals the reservoir. This allows for pressurized argon to fill the reservoir, pushing lithium into the feed system to prime the $\mathbf{J} \times \mathbf{B}$ pump.

G. Assembled Feed System

Assembling all of the feed system components, photos of the $\mathbf{J} \times \mathbf{B}$ feed system are shown in Figure 9. In photo A, the feed system is shown installed in the vacuum chamber. The entire feed system is attached to a large aluminum block to allow the feed system to fit within the chamber and to raise the top of the

reservoir to the height of the thruster. This assembly is mounted to the thruster table. Photo B shows the $\mathbf{J} \times \mathbf{B}$ pump with the magnet assembly and heater blocks in place.

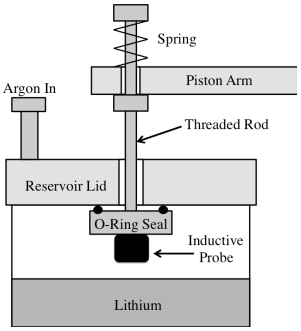

Figure 8. During operation the inductive proximity detector backplate is made to press against the reservoir lid. A spring at the top of the threaded rod then compresses to form an upward force on the O-ring, forming an a seal.

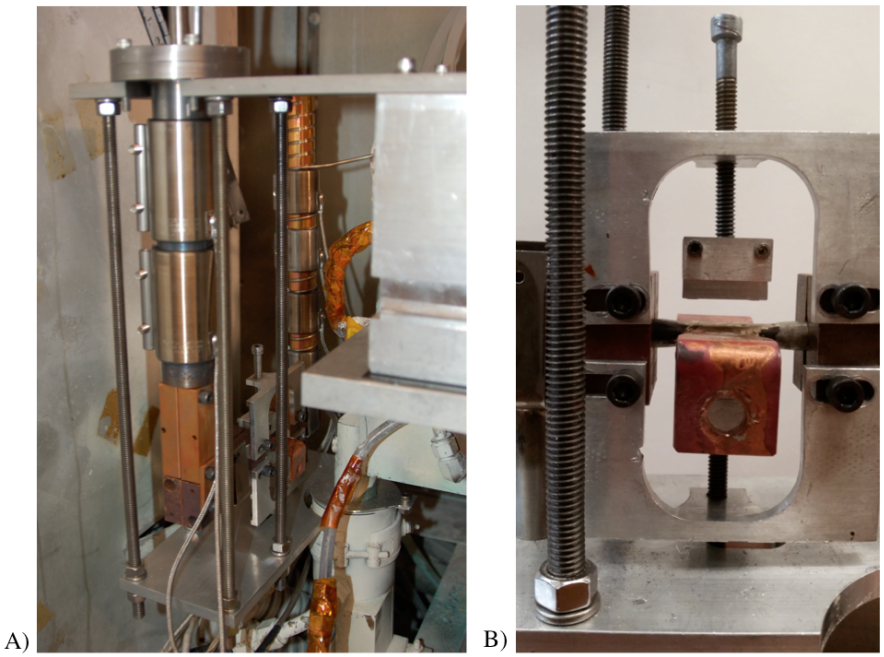

Figure 9. In photo A, the $\mathbf{J} \times \mathbf{B}$ pump feed system is mounted to a large aluminum block within the vacuum chamber and fixed to the thruster table surface. This configuration allows the system to fit into the vacuum chamber and lifts the top of the reservoir to the height of the thruster. In photo B, the $\mathbf{J} \times \mathbf{B}$ pump is shown within the new feed system. The pump was made using a flattened length of 3/8" stainless steel tubing with two copper electrodes braised to the body. The permanent magnets are housed in aluminum and can be raised or lowered to obtain a desired magnetic field strength at the pump.

III. Results

With a successful demonstration of the measurement system, trials pumping liquid lithium in the $\mathbf{J} \times \mathbf{B}$ feed system were performed. A calibration of the proximity detector's voltage response in the presence of the liquid metal surface was taken and is shown in Figure 10. The calibration recorded a detection range of 1.2 mm under operating conditions. In Figure 11, a fit was made to this calibration data and used to calculate the distance to the lithium surface with an uncertainty of $\pm$ 0.003 mm height corresponding to an uncertainty in mass of $\pm$ 1.46 mg.

After priming the $\mathbf{J} \times \mathbf{B}$ pump using argon pressure, current was delivered to the pump. Due to significant

vibration from an adjacent vacuum pump, the proximity detector recorded a large sinusoidal voltage with a frequency of ~ 3 Hz. A low-pass filter was applied to this raw data, and the filtered detector voltage is shown in Figure 12. In this figure, a clear increase in the detector voltage is seen with the pump operating at full current. The rise in the voltage corresponds to the lithium column height decreasing and was accompanied by slowly growing droplets of lithium at the tubing exit.

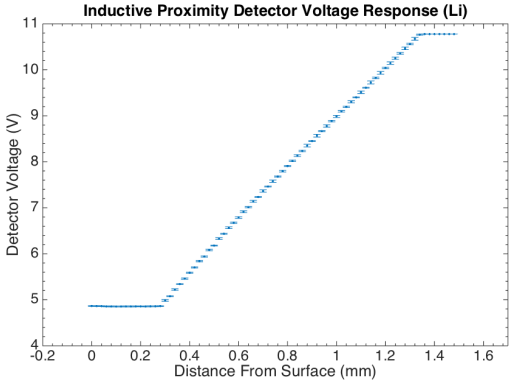

Figure 10. Similar to the calibration done on the aluminum surface, a voltage response was taken using liquid lithium in the feed system reservoir at 200°C. The proximity detector's full range of detection is about 1.2 mm.

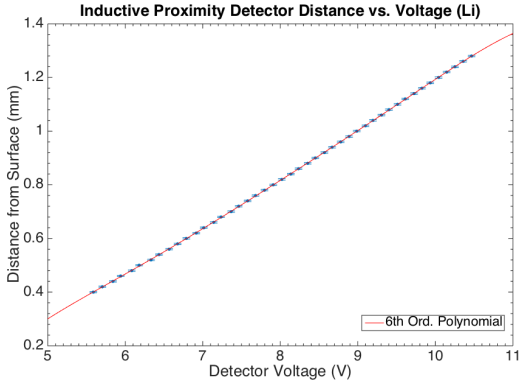

Figure 11. As with aluminum a sixth-order polynomial fit was made between 5.5 - 10.5 V. Here, the uncertainty in the position is measured to be $\pm$ 0.003 mm corresponding to a mass uncertainty of $\pm$ 1.46 mg.

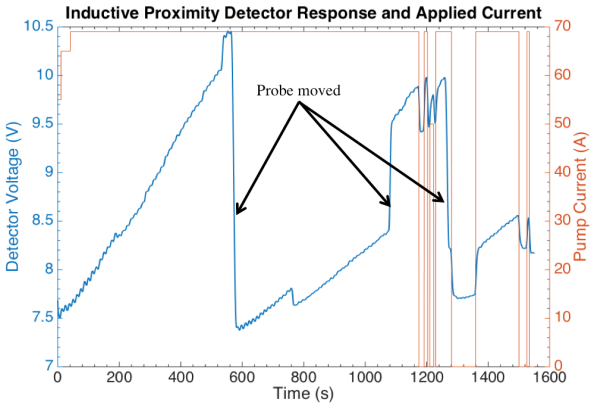

Figure 12. An increasing voltage was observed indicating that lithium column height was decreasing. After moving the piston to keep the proximity detector within its sensing range, this rising voltage was still observed with an interruption in pumping at 750 s corresponding to the brief solidification of the droplet at the tubing exit.

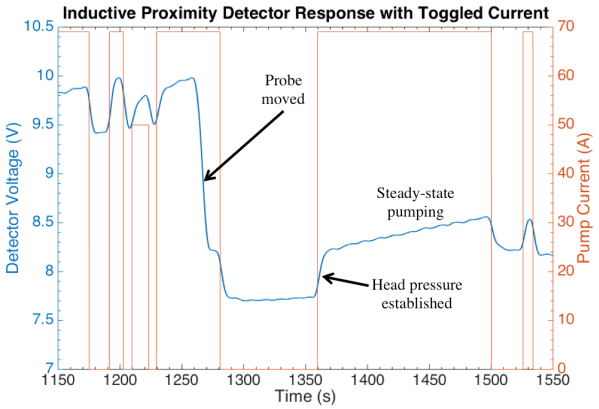

Figure 13. The pump current was toggled on and off be sure that the changing voltage and dripping was indeed correlated to the pump being turned on. When turned on, as at 1360 s, a sharp rise in voltage corresponds to the pump establishing a head pressure before entering a steady-state pumping mode.

As the rise in voltage took place over a long timescale, the current to the pump was toggled on and off as shown in Figure 13 to be sure that this voltage rise was due to the effects of the pump. At different stationary heights, a clear rise in the voltage was only seen when the pump was toggled on. When current is applied to the pump, a sharp rise in voltage is initially observed due to the pump establishing a head pressure before continuing to steady-state pumping.

Figure 14 shows six regions chosen for a series of linear fits including region 5 where no pump current was applied. In Figure 15, an appropriate linear fit window of 25 s was determined, and the mass flow rate in each region was calculated with a measurement uncertainty of $\pm$ 0.03 mg/s. When operated at maximum current, the pump provided a mass flow rate between $\sim$ 0.1-0.7 mg/s with considerable variation within each region.

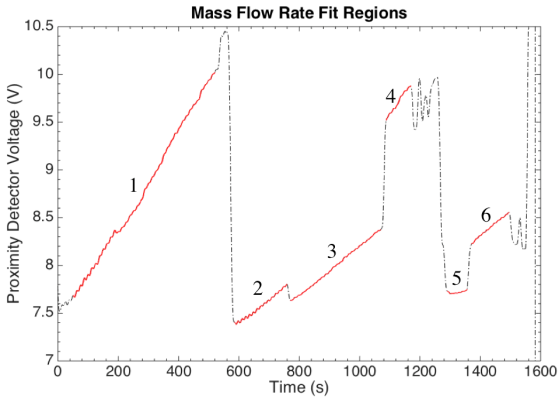

Figure 14. To measure the mass flow rate generated by the J × B pump, six regions were chose for a sliding linear fit. After using the proximity detector calibration curve to translate into mass data, the slope of these linear fits correspond to the mass flow rate. No current is provided to the pump in region 5 and is included as a source of comparison.

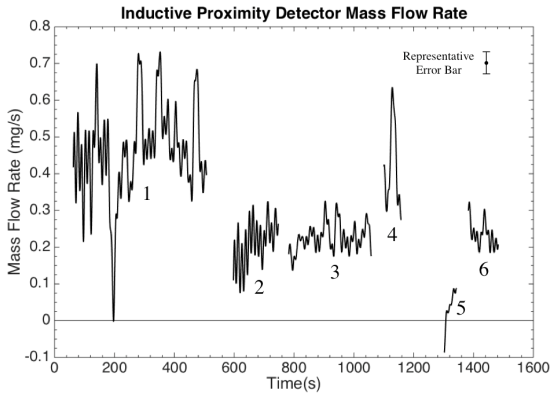

Figure 15. A 25 s sliding linear fit was performed on each of the regions shown in Figure 14 with an uncertainty of ± 0.03 mg/s. Despite the pump being run at the same current in regions 1 - 4 and 6, two distinct mass flow rates of ∼ 0.46 mg/s and ∼ 0.21 mg/s were observed due to a skin of solid lithium forming on the droplets at the tubing exit. No pump current was applied in region 5.

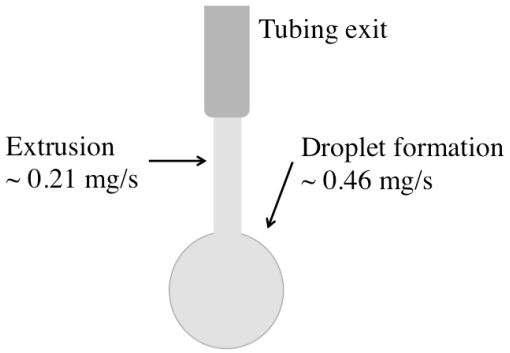

Figure 16. Due to inadequate heating at the tubing exit, a skin of solidified lithium formed at the surface of the droplet and a mass flow rate of ∼ 0.46 mg/s was measured. After sufficient cooling, the droplet ceased to grow, and a thin extrusion lithium formed corresponding to a mass flow rate of ∼ 0.21 mg/s. The presence of this solidification impeded the flow of liquid lithium, and caused variation in the mass flow rate.

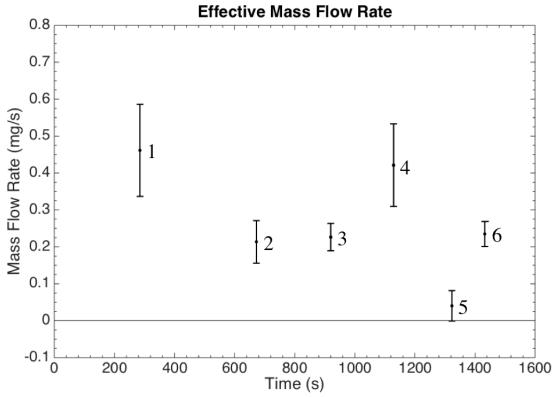

Figure 17. As the mass flow rate and thus total change in column height was quite small, the expected mass flow rate was assumed to be constant for each fit region. The average mass flow rate and standard deviation in the flow rate was then taken for each of these regions. The considerable variation in mass flow rate for each region is primarily due to the solidification of lithium at the tubing exit.

This variation in mass flow rate was caused by solidification of the droplet surface at the tubing exit. Despite the presence of a heater at the tip and a tank pressure of ∼ 1 mTorr, surface discoloring and solidification was observed on the lithium droplet and affected the maximum mass flow rate and variation in each fit region. In regions 1 - 4 and 6, two distinct mass flow rates of ∼ 0.46 mg/s in region 1 and 4, and ∼ 0.21 mg/s in regions 2, 3, and 6 were observed. As shown in Figure 16, the higher mass flow rate was observed as the lithium droplet formed. However, as this droplet formed, a skin of solid lithium formed at the surface, impeding and varying the flow of lithium. After sufficient cooling, the droplet stopped growing and a thin extrusion of solid lithium was formed at the exit, corresponding to the lower mass flow rates. Both mass flow rates were distinguishably higher than region 5 when no current was provided to the pump.

An effective mass flow rate was calculated for each region and plotted in Figure 17. A range of ∼ 0.2 - 0.5 mg/s was measured with an average variation of ± 0.08 mg/s in the achieved mass flow rate. A maximum

effective mass flow rate of 0.46 ± 0.13 mg/s was found in region 1.

One final analysis was to determine a more accurate measure of the effective viscosity. While the system was originally designed to operate from 0 - 100 mg/s, the experimental mass flow rate was much smaller than expected. Using a maximum current value of 58 A and mass flow rate of 0.46 mg/s, one can instead solve Eq. 5 for the effective viscosity finding a value $\mu = 0.107$ Pa·s, a factor of about 180 times greater than the reference value used to initially design the feed system. By accounting for the addition of surface tension in Eq. 3, a maximum mass flow rate of 40 mg/s is expected for the current feed system configuration. This is still far above the measured mass flow rate, and the solidification of the lithium droplets is suspected as the primary source of the reduced and noisy mass flow rate. Future tests with additional heating will be carried out and are anticipated to both dramatically increase the maximum mass flow rate, and reduce the variation in the mass flow rate. When connected to the cathode, lithium at the feed system exit will be vaporized, eliminating the issues of solidification and surface tension. Simple modifications to the tubing length and magnetic field strength can then be made to obtain the desired range of mass flow rates.

IV. Conclusion

In this paper, we have presented a new $\mathbf{J} \times \mathbf{B}$ feed system design to deliver liquid metals in the mg/s flow regime. A process for determining relevant system parameters was presented and calculated for the mass flow rate regime of 0 - 100 mg/s and available power supply currents of 0 - 70 A at a resolution of 100 mA. Using a simplified $\mathbf{J} \times \mathbf{B}$ pump design with variable magnetic field strengths, this feed system was then validated using a translating inductive proximity detector and control program to track the changing height of the liquid column height in the reservoir.

The full feed system was tested using liquid lithium. Calibrations of the proximity detector were conducted, and the $\mathbf{J} \times \mathbf{B}$ pump was successfully operated. Using the inductive proximity detector, we measured mass flow rates of 0.2 - 0.5 mg/s with a measurement uncertainty of ± 0.03 mg/s, and achieved a maximum effective mass flow rate of 0.46 ± 0.13 mg/s. As the maximum mass flow rate detected was much smaller than that predicted, the effective viscosity of the system was calculated and found to be $\mu = 0.107$ Pa·s which is two orders of magnitude greater than the reference value and attributed to solidification at the tubing exit. Future tests will incorporate more heating at the exit and is anticipated to dramatically increase the mass flow rate range. Simple modifications to the tubing length and magnetic field strength can then be used to achieve the desired range of mass flow rates.

V. Acknowledgements

This research was conducted with support from the Program in Plasma Science and Technology through the Princeton Plasma Physics Laboratory. We are grateful to Bob Sorenson for his technical assistance in the design and development of the feed system. We would also like to thank previous undergraduate students who have contributed to this project including Nicolas Luzarraga, Jeremy Mehl, and Brannon Jones.

References

[1]Polzin, K. A. and Markusic, T. E., "Electromagnetic Pumps for Liquid Metal-Fed Electric Thrusters," Journal of Propulsion and Power, Vol. 23, No. 6, 1285-1290, 2007.

[2]Polzin, K. A.,Markusic, K. E., Stanojev, B. J., Dodson, C. and DeHoyos, A.,"Electromagnetic Flow Sensor for Liquid-Metal-Fed Electric Propulsion," Journal of Propulsion and Power, Vol. 24, No. 5, 2008.

[3]Kodys, A. D. et al., "Lithium Mass Flow Control for High Power Lorentz Force Accelerators," AIP Conference Proceedings, Vol. 552, Albuquerque, NM, 11-14 Feb. 2001.

[4]White, F. M., "Fluid Mechanics," Viscous Flow in Ducts, 6th ed., McGraw Hill, New York, 2008, pp. 364.

[5]Davidson, H., "Compilation of Thermophysical Properties of Liquid Lithium," NASA Technical Note, D-6450, 1968.

[6]Mehl, J., "Design and Testing of a Propellant Feed System for the Lithium Lorentz Force Accelerator," Undergraduate Thesis, Princeton University, 2015.